Published in final edited form as:
Cancer Res. 2012 June 1; 72(11): 2791–2801. doi:10.1158/0008-5472.CAN-12-0320.

Inhibiting Autophagy During Interleukin 2 (IL-2) Immunotherapy Promotes Long Term Tumor Regression

Xiaoyan Liang[1], **Michael E. De Vera**[1], **William J. Buchser**[1], **Antonio Romo de Vivar Chavez**[1], **Patricia Loughran**[1,2], **Donna Beer Stolz**[2], **Per Basse**[3], **Tao Wang**[4], **Bennett Van Houten**[4], **Herbert J. Zeh**[1], and **Michael T. Lotze**[1,3]

[1]Department of Surgery, University of Pittsburgh Cancer Institute, 5117 Centre Avenue, Pittsburgh PA, 15213

[2]Center for Biologic Imaging, University of Pittsburgh

[3]Department of Immunology, University of Pittsburgh

[4]UPCI Molecular and Cellular Biology Program. University of Pittsburgh

Abstract

Administration of high dose interleukin 2 (HDIL-2) has durable antitumor effects in 5-10% patients with melanoma and renal cell carcinoma. However, treatment is often limited by side effects, including reversible, multi-organ dysfunction and characterized by a cytokine-induced 'systemic autophagic syndrome'. Here we hypothesized that the autophagy inhibitor chloroquine (CQ) would enhance IL-2 immunotherapeutic efficacy and limit toxicity. In an advanced murine metastatic liver tumor model, IL-2 inhibited tumor growth in a dose-dependent fashion, and these anti-tumor effects were significantly enhanced upon addition of CQ. The combination of IL-2 with CQ increased long term survival, decreased toxicity associated with vascular leakage, and enhanced immune cell proliferation and infiltration in the liver and spleen. HDIL-2 alone increased serum levels of IFN-γ, IL-6 and IL-18 and also induced autophagy within the liver and translocation of HMGB1 from the nucleus to the cytosol in hepatocytes, effects that were inhibited by combined administration with CQ. In tumor cells, CQ increased autophagic vacuoles and LC3-II levels inhibited oxidative phosphorylation and ATP production and promoted apoptosis, which was associated with increased Annexin V^+/PI^- cells, cleaved-PARP, cleaved-caspase 3, and cytochrome C release from mitochondria. Taken together, our findings provide a novel clinical strategy to enhance the efficacy of HDIL-2 immunotherapy for cancer patients.

Keywords

Autophagy; Interleukin 2; HMGB1; oxidative phosphorylation; tumor metabolism; apoptosis

Corresponding Authors: 1. Michael T Lotze, MD or Xiaoyan Liang MD. PhD 5117 Centre Ave Room G.27 Pittsburgh Pa, 15232 412-623-1211, 412-623-1212 lotzemt@upmc.eduliangx@upmc.edu 2. Michael E. De Vera MD Current address: 25865 Barton Rd Suite 101 Transplantation Institute Loma Linda University Loma Linda, CA. 92354 909-558-3650 medevera@llu.edu.

Precis: The preclinical study shows how the inexpensive autophagy inhibitor chloroquine might be repositioned to greatly enhance the antitumor effects of IL-2, a central growth and survival factor for T cells used for melanoma treatment, while limiting the toxicity that has its restricted its broad use in clinic.

Conflict of Interest: None

Conventions: IL-2, HMGB1, LC3, OXPHOS

Introduction

Two decades ago, recombinant interleukin 2 received FDA approval for the treatment of patients with advanced renal cancer and subsequently of patients with melanoma. High dose IL-2 (HDIL-2) administration is associated with an objective 25% response rate in patients with kidney cancer, as reported in the recently completed IL-2 SELECT trial (1). Almost 20% of these patients survive more than 5 years (2-4). Attempts to improve the response rate and/or limit toxicity of IL-2 administration by inhibiting TNF, iNOS, or VEGF have failed. Combination with IFN-α administration did not improve outcome appreciably (2, 3). Other efforts including vaccination (5), adoptive cellular therapies (6) and CTLA-4 inhibition (7, 8) are associated with both increased efficacy and toxicity. HDIL-2 administration remains the only agent with proven efficacy in producing durable complete and partial responses in patients with metastatic renal cell carcinoma (RCC) (9).

The greatest limitation of IL-2 treatment has been the associated side effects including hypotension as well as cardiac, gastrointestinal, renal, cerebral, pulmonary, and hepatic toxicity. These adverse effects are occasionally life threatening, and treatment is usually restricted to specialized centers, often resulting in early discontinuation or interruption of treatment (10, 11). The precise mechanism mediating these side effects has not been clear. We have proposed that IL-2 toxicity is due to a cytokine-induced ‘systemic autophagic syndrome’. Recently, several cytokines including Type II interferon and transforming growth factor beta (TGFβ) have been shown to induce autophagy (12). We hypothesized that the systemic syndrome associated with IL-2 treatment was related to cytokine-induced autophagy and temporally limited tissue dysfunction. The use of the autophagy inhibitor, chloroquine (CQ) could limit toxicity and thereby enhance efficacy.

Autophagy is a tightly regulated catabolic process involving the degradation of cellular components through the lysosomal machinery and plays a central role in cell growth, development and homeostasis (13). The role of autophagy in cancer is complex and context dependent. In normal tissues, autophagy is an important tumor suppressor pathway that limits oxidative stress and tissue damage that can promote cancer initiation during periods of excessive apoptotic cell death and inflammation. Autophagy, however, also supports cellular metabolism that has the potential to aid the growth of advanced tumors with increased metabolic demands following an ‘autophagic switch’ (14) in developing tumors. In an established tumor, cells are exposed to perpetual hypoxia, acidosis and nutrient deprivation. Increased autophagic flux enables adaptation to the hypoxic and nutrient-limited microenvironment. Increased autophagy is observed clinically in late-stage colon cancer, breast cancer, melanoma, hepatoma and malignant glioma (15-19). Enhanced immune responses to tumors have been observed when hypoxia-induced autophagy is inhibited by chloroquine treatment (20). Autophagy promotes metastasis in some circumstances, enhancing tumor cell fitness in response to environmental stress (21).

Several studies have suggested that autophagy may act as a protective mechanism in tumor cells in which cell death is induced by chemotherapy, immunotherapy, or radiotherapy (20, 22-25). Targeting autophagy has increased the antitumor effects of individuals anticancer therapies in preclinical trials (13). There has been very limited exploration of autophagy inhibition therapy in combination with biologic therapy (20, 26).

Chloroquine (CQ) was used for many years as an anti-malarial but is now used most commonly in patients with rheumatoid arthritis and systemic lupus erythematosus. It inhibits autophagy by blocking acidification of the lysosome, preventing fusion with the autophagosome (23). This results in decreased degradation of autophagosomes, eventuating in either apoptotic or necrotic cell death. CQ has extensive biological effects, inhibiting

cellular proliferation and/or inducing cell apoptosis in human and murine tumor cell lines (24, 27). Induction of apoptosis is associated with the loss of mitochondrial membrane potential, release of cytochrome c, activation of caspase-9 and caspase-3, and cleavage of poly(ADP-ribose) polymerase. *In vivo*, CQ significantly inhibits 4T1 colorectal cancer growth and metastasis in murine models and induces apoptosis within the tumor micro-environment (28). Studies of human (24, 29) and murine cancer cell lines (30) suggest that CQ may exert significant antitumor activity by inhibiting the induction of autophagy following cancer therapy. We hypothesized that inhibition of autophagy with CQ in combination with HDIL-2 treatment would increase antitumor effects and promote survival when compared with IL-2 administration alone, enabling more effective expansion and function of immune cells.

MATERIALS AND METHODS

Animals and Tumor Cell Lines

Female C57BL/6 (B6, H-2^b) mice, 8-10 weeks old, were purchased from Taconic (Germantown, NY). Animals were maintained in a specific pathogen-free facility at the University of Pittsburgh Cancer Institute, and used in accordance with institutional and National Institutes of Health guidelines. MC38 murine colorectal carcinoma and Panc-02 adenocarcinoma cells (C57BL/6 syngeneic) were purchased from The American Type Culture Collection (ATCC). RENCA renal cell cancer and B16 melanoma cell lines were gifts from Dr. W. Storkus at the University of Pittsburgh. All these cell lines were authenticated using genomic profiling in March 2012 (IDEX Radil Cell Check, MO). Cells were maintained in DMEM medium supplemented with 5% heat-inactivated FBS, 2 mM L-glutamine, 100 U/ml penicillin, 100 mg/ml streptomycin, 0.1 mM nonessential amino acids, and 1 mM sodium pyruvate.

Liver Metastasis Model

Liver metastases were obtained by direct portal injection of tumor cells as described previously (31). Briefly, mice were anesthetized with a single intraperitoneal injection of Ketamine (50 mg/kg, NLS animal Health, Owing Mills, MD) and Xylazine (10 mg/kg, NLS animal Health, Owing Mills, MD). The portal vein was exposed through a small midline incision. 2×10^5 luciferase transfected tumor cells suspended in 200 μl normal saline (NS) were injected. The incision is closed with vycryl suture. Seven days following tumor inoculation, mice were randomized into 6 groups and received their first bioluminescence imaging (BLI) measurement, then started receiving intraperitoneal injection of rIL-2 with or without combination of CQ. Clinical grade rIL-2 was a kind gift of Prometheus Laboratories Inc. (San Diego, CA, USA). Untreated control mice (UT) were injected with a comparable amount of NS on the same schedule. Tumor burden was assessed with the IVIS bioluminescence image described below. Blood was collected by direct intracardiac puncture and spleens and livers were harvested for electron microscopy, confocal imaging, and isolation of immune cells.

Luciferase Transfection of Tumor Cells and Bioluminescence Imaging (BLI)

Stably transduced tumor cells expressing the firefly luciferase gene were generated by lentiviral transfection of the pGL4 Luciferase Reporter Vector (Promega, Madison) and selected with puromycin. Growth characteristics and phenotype of the transfected cells were compared with the parental strain *in vitro* to verify the absence of any effects secondary to retroviral insertion. Prior to imaging, mice were anesthetized by Isoflurane (Wester Veterinary, Sterling, MA) inhalation followed by intraperitoneal injection of luciferin (300 mg/kg, Caliper Life Sciences, Hopkinton, MA). After waiting 8 minutes to allow proper distribution of luciferin, the mice were imaged using an IVIS 200 system (Xenogen

Corporation, Hopkinton, MA) according to the manufacturer's instructions. Living Image software (Xenogen) was used to analyze the resultant data. Regions of interest were manually selected and quantification is reported as the average of photon flux within regions of interest. The BLI signal is represented as photons/second/cm^2/steradian.

Isolation of Non-parenchymal Cells and Flow Cytometry

Mouse livers were messed and digested 1% collagenase (Sigma, St. Louis, MO) solution at 37°C for 30 minutes. To obtain adequate numbers of non-parenchymal cells, livers from three to five animals were combined from each treatment group. The non-parenchymal cells were then isolated by centrifugation over a Percoll gradient (Sigma Chemical Co., St Louis, MO). Cell surface antigen expression was analyzed by flow cytometry (Becton Dickinson FACScan) using FITC or PE conjugated monoclonal antibodies against mouse CD11c, CD14, CD19, CD4, CD8, Gr-1, and NK1.1 (all from BD Pharmingen, San Diego, CA). Appropriate isotype and species-matched irrelevant monoclonal antibodies were used as controls.

Serum Cytokine Determination

Blood was collected from direct intracardiac puncture at individual intervals following tumor inoculation. Serum was used to measure HMGB1 (Shinotest, Japan), IL-6, IL-18, and IFN-γ (R&D, Minneapolis, MN) levels by ELISA.

Detection of Apoptosis

MC38 tumor cells (2×10^5 /ml) were cultured in 24-well plates and treated with CQ for 4 or 24 hours. Cells were then harvested and stained with Annexin V and propidium iodide (PI) (BD Pharmingen) according to the manufacturer's protocol. Quantitative analysis was performed by flow cytometry, with 10,000 events acquired from each sample.

Immunofluorescence Staining

A portion of each lobe of the liver was embedded in OCT Compound (Miles, Elkhart, IN), frozen, and stored at -80°C. Cryostat sections (8 μm) were used for immunofluorescence evaluation. *In vitro*, tumor cells were cultured in eight - chamber slides, treated with 100 to 200 μM CQ for 4 and 24 hours, fixed with 2% PFA 30 minutes, and prepared for immunofluorescence staining. The following primary monoclonal antibodies were used: rabbit anti-human HMGB1 (R&D) and rabbit anti-LC3 (Novus Biologicals Inc. CO), rabbit-TOM-20 and mouse anti-cytochrome C (Santa Cruz Biotechnology Inc, Santa Cruz, CA). Slides were incubated with the primary antibody overnight at 4°C. Following three washes in PBS, slides were incubated with fluorescent-conjugated secondary antibodies for 45 minutes followed by Hoechst nuclear staining. Negative controls included staining with the corresponding isotype for each antibody and staining with secondary antibody alone. Positive controls included immunostaining of known positive tissues.

Protein Blot Analysis

Whole-cell lysates were resolved on 10% SDS-PAGE gel and transferred to 0.2 μm nitrocellulose membranes. After blocking, membranes were incubated overnight at 4°C with primary antibodies specific for cleaved-PARP (Cell Signaling, Danvers, MA), caspase-3, (Assay designs Inc, Ann Arbor, MI), LC-3 (Novus Biologicals, CO), cytochrome C (Santa Cruz, Santa Cruz, CA), and β-actin (Sigma, St Louis, MO). After incubation with peroxidase-conjugated secondary antibodies for 1 h at 25°C, membranes were developed with the SuperSignal West Pico chemiluminescence kit (Pierce, Rockford, IL) and exposed to film. Image J was used to quantify the bands.

Statistical Analyses—Statistical significance was assessed using the Student's *t*-test, Mann-Whitney U test, or ANOVA when appropriate using SPSS 16.0 (SPSS, Chicago, IL) or Spotfire DecisionSite (Tibco, Palo Alto, Ca). A p-value < 0.05 was considered significant. All experiments reported here were repeated at least two or three times with similar results with representative findings presented.

Transmission electron microscopy (TEM)(32, 33), ATP Quantification, and *XF Bioenergetic Assay* were used and are described in supplemental materials.

Results

Chloroquine, in combination with HDIL-2, promotes profound anti-tumor effects, enhancing murine survival in a liver metastasis model

In preliminary experiments, we confirmed that rIL-2 inhibited tumor growth in a dose dependent fashion (Supplemental Figure 1) in a murine liver metastasis tumor model that we have developed. Although administration of 600,000 IU/mouse rIL-2 twice a day can inhibit tumor growth, many of these mice subsequently progress (Figure 1 A and B). Administration of high dose rIL-2 results in life-threatening systemic toxicity which precluded administration of higher doses. We hypothesized that these adverse effects may be related to the widespread induction of systemic autophagy. Therefore, we sought to determine the effects of administration of autophagy inhibitor agent CQ both alone and in combination with IL-2, in a hepatic metastatic tumor model.

Mice received 2×10^5 luciferase-labeled mouse colorectal cancer MC38 cells via portal vein injection. Seven days later, they were randomly divided into 6 groups that received vehicle control (UT), CQ alone 50mg/kg/day for 30 days, rIL-2 60,000 (low dose IL-2, LDIL-2) or 600,000 IU/mouse (HDIL-2), twice a day for 5 day, with or without combination of CQ. Tumor growth was measured by BLI (Figure 1A and B) and survival of mice was determined (Figure 1D and Table 1). We found that 50mg/kg CQ alone only had a modest but insignificant effect in inhibiting tumor growth (p=0.44). In the UT control group, median survival was 31 days and the longest survival time was 55 days. IL-2 administration inhibited tumor growth in a dose dependent manner. Low dose IL-2 only modestly inhibited, while HDIL-2 significantly inhibited tumor growth, prolonging the resultant survival time (p<0.01). The median survival in the HDIL-2 group was 135 days and 44.4% of animals were tumor free, surviving longer than 150 days.

A dramatic effect on tumor growth was noted when CQ was administered in combination with HDIL-2. Although BLI revealed visible tumors in all five mice on day 7 prior to treatment in the liver (Figure 1A and 1B), after 5 days of HDIL-2 and CQ combination treatment, only one mouse developed tumor while the others were completely eradicated (90% of animals) and survived without tumor for over 150 days (Table 1). Comparing the survival curves in these two groups reveals a significant difference (p=0.024). These results suggest that the combination strategy of HDIL-2 and CQ was extraordinarily effective with almost complete elimination of tumors (Figure 1A). Similar anti-tumor effects of IL-2 were observed with treatment of the pancreatic cancer cell line Panc02 in the hepatic tumor model (Supplemental Figure 2) as well as the Renca tumor in Balb/c mice (Supplemental Figure 3). The B16 melanoma pulmonary metastases model was not susceptible to IL-2 alone (as shown previously by us and others) or in combination with CQ (data not shown).

In the clinic, one of the primary adverse effects of HDIL-2 therapy is the vascular leak syndrome resulting in fluid retention associated with increased body weight. In order to assess HDIL-2 toxicity, murine body weight was measured before and every other day during treatment. Although handling of mice receiving saline control typically is associated

with initial weight loss, administration of HDIL-2 increased body weight, and this effect was prevented by combination with CQ ($p<0.05$) (Figure 1C). Serum chemistry analysis suggested that 600,000IU IL-2 twice a day did not result in significant liver or kidney dysfunction (Supplemental Table 1), unlike that observed in patients.

HDIL-2 administration induces inflammatory cytokine release which is inhibited by CQ

Our previous findings indicated that HMGB1 plays an important role in regulation of autophagy and apoptosis in tumor cells. Translocation from the nucleus into the cytosol is associated with release of HMGB1 into the serum (33). Systemic release of HMGB1 may be related to the induction of systemic autophagy within tissues or cells which are in turn associated with the toxicity of HDIL-2. We assessed HMGB1 distribution *in situ* in the liver as well as its serum level. Two hours following the last the dose of HDIL-2 treatment (day 12 following tumor inoculation), liver tissues and serum were harvested. HMGB1 distribution *in vivo*, and liver tissue immunofluorescence staining showed that HMGB1 was present predominately in the nuclei of hepatocytes in untreated animals, as we have previously reported (31), but primarily located in the cytosol of hepatocytes in HDIL-2 treated animals with an HMGB1 staining void within nuclei. Combination of CQ prevented HMGB1 translocation (Figure 2A). This result is consistent with the change of HMGB1 serum levels in mice under different treatments. When compared with sham animals, tumor injection temporarily increases serum HMGB1 levels within 24 h following tumor intraportal delivery which then returns to normal levels (31). When compared with the UT control group, serum HMGB1 levels were significantly increased in animals receiving HD IL-2 treatment ($p<0.05$) (Figure 2B). Conversely, combinations of CQ with IL-2 significantly decreased HMGB1 serum levels when compared with HDIL-2 alone ($p<0.05$). These results suggest that CQ may limit HDIL-2 induced HMGB1 release thereby decreasing the associated systemic toxicity. CQ administration alone did not change the serum levels of HMGB1.

Similar results were observed with other inflammatory cytokines. Compared with untreated control, HDIL-2 significantly increased levels of IL-6, IL-18 and IFN-γ in the serum. Administration of CQ inhibited levels of all cytokines except IL-18, which increased slightly. Thus the “cytokine storm” associated with the systemic toxicity of HDIL-2 were at least partially inhibited by CQ administration.

HDIL-2 significantly enhances immune cell proliferation and infiltration within the liver and spleen

Two hours following the last dose of HDIL-2 injection twice daily for five days, liver non-parenchymal cells and splenocytes were isolated, counted and analyzed by flow cytometry. Consistent with our previous study, intrahepatic leukocyte numbers and splenocyte numbers were not changed following intraportal infusion of MC38 tumor cells (31) but significantly increased by administration of HDIL-2. Flow cytometric analysis suggested that HDIL-2 significantly increased $CD11c^+$, $CD4^+$, $CD8^+$, and $CD11b^+$ cells (Figure 3A, $p<0.004$). Combination of IL-2 and CQ further enhanced this effect. There was also a modest elevation of $Gr\text{-}1^+/CD11b^+$ cells and $CD4^+/CD25^+$ cells as well as CD8+ cells ($p<0.05$, Figure 3B).

HDIL-2 administration induces profound mitochondrial changes and heightened autophagy

To assess the systemic effects of HDIL-2, (1.5×10^6 IU IL2 BID) was administered and liver and kidney tissues from individual groups of mice were harvested and processed for TEM. When compared with UT animals, hepatocyte mitochondria from IL-2 treated mice had disrupted outer mitochondrial membranes and absent or disordered mitochondrial christae. This could be a consequence of membrane provision to rapidly generate autophagosomes as

has been reported in the setting of starvation (34) or a reaction to toxic reactive oxygen species generated during IL-2 induced stress. Increased endoplasmic reticulum (ER) surrounding the altered mitochondria were also visualized. The ultrastructure of the kidney proximal and distal tubule cells from both control and treated mice appeared normal (Figure 4A). Furthermore, liver and kidney tissue lysates were collected from tumor bearing mice that received IL-2 alone or in combination with CQ on the day following the last dose of IL-2. HDIL-2 treatment increased the apparent level of autophagic flux with enhanced conversion of LC3-I to LC3-II in the liver but not within the kidney tissue lysates, suggesting resistance of some tissues to the induction of autophagy. CQ blocks the formation of autolysosomes, inhibiting the final steps of the autophagic process (35). Administration of CQ further enhances LC3-I/II levels in both groups of mice receiving CQ alone or in combination with IL-2. Enhancement of visualized autophagic vacuoles (termed autophagosomes) in treated animals were not observed (Figure 4B).

Chloroquine inhibits autophagic flux in tumor cells

To determine whether CQ causes a similar effect on tumor cells, LC3 punctae were assessed in both MC38 and Panc02 cells. When compared with the untreated controls, CQ-treated tumor cells exhibited intense LC3 punctae by immunofluorescent staining (Figure 5A). Under TEM, tumor cells appeared to have lost visible mitochondria and rough endoplasmic reticulum while accumulating autophagic vacuoles (AV) within the cytosol (Figure 5B). To confirm these immune-cytochemical observations, western blots were performed on whole cell lysates collected at 4 h following treatment with either 100 or 200 μM CQ and the level of LC3-I and LC3-II assessed. A dose dependent increase of LC3-II was observed in both MC38 and Panc02 cells (Figure 5C). These results suggest that CQ induces accumulation of AV, inhibiting autophagic flux in both tumor cell lines.

Chloroquine treatment alters tumor cell metabolism

With TEM, in addition to accumulated AVs, we also found altered mitochondria which have disrupted outer membrane and disordered mitochondrial christae (arrow) in CQ- treated tumor cells (Supplemental Figure 4). This suggested that CQ may alter tumor cell metabolism. Cells synthesize ATP solely through two pathways, mitochondrial respiration (oxidative phosphorylation, OXPHOS) and glycolysis. OXPHOS is more efficient, accounting for 90% of the ATP synthesized within normal cells. According to the Warburg hypothesis (36), tumor cells are surprisingly more dependent on glycolysis even in the presence of adequate oxygen and nutrients. In ATP production studies, blockade of glycolysis with 2-DG in MC38 and Panc02 tumor cells significantly diminished ATP levels but did not change when OXPHOS was blocked by oligomycin and rotenone (Supplemental Figure 5) This has been attributed to both the need for substrate for anabolism and cell division (37) as well as the requirement of more rapid ATP generation by glycolysis in the setting of cell stress.

To demonstrate that CQ alters tumor cell metabolism, an XF bioenergetic assay system was employed to explore the effects of CQ treatment on the bioenergetic phenotype of MC38 tumor cells by real-time monitoring of mitochondrial respiration in which oxidative phosphorylation (OXPHOS) is measured by oxygen consumption rate (OCR) while glycolysis is measured by the generation of lactate and the consequent extracellular acidification rate (ECAR). MC38 cells were exposed to 100 μM CQ for 4 hr after which the effects of successive addition of oligomycin, FCCP, 2- Deoxy-D-glucose (2-DG), and rotenone, OXPHOS and glycolysis rates were measured in real time. CQ significantly decreased baseline OCR in a dose-dependent fashion (Figure 6A, B) but had no effect on baseline ECAR (data not shown). The addition of the Complex V inhibitor, oligomycin, resulted in similar decrease in OCR with or without CQ addition. The mitochondrial

uncoupler, FCCP, restored OXPHOS to levels above the baseline. 2-DG is a glucose analog that inhibits hexokinase, the first enzyme in the glycolysis pathway, converting glucose to glucose-6-phosphate. Blockade of glycolysis by addition of 2-DG raised OCR slightly within control tumor cells because of OXPHOS compensation while the presence of CQ inhibited this effect. Addition of the Complex I inhibitor rotenone significantly decreased both OCR and ECAR. These studies demonstrate that CQ decreases both OXPHOS and glycolysis within MC38 tumor cells, promoting a metabolic death. The agent ethyl pyruvate, which we have shown has antitumor activity and limits HMGB1 release, increased oxidative phosphorylation (Supplemental Figure 6), suggesting that the OXPHOS decrease is not a generalizable phenomenon attributable to antitumor compounds.

As OXPHOS and glycolysis constitute the sole energy source of tumor cells, ATP levels were measured in the presence or absence of chloroquine. We found that ATP levels were markedly diminished following a short term increase that may have resulted from compensatory increases in OXPHOS (Figure 6C).

Chloroquine treatment induces tumor cell apoptosis

CQ directly inhibits CT26 proliferation by inducing apoptosis both *in vitro* and *in vivo* (24). We demonstrated that CQ inhibits MC38 and Panc02 cell proliferation and survival. The role of autophagy in tumor cell survival has not been elucidated completely, and the relationship between autophagy and apoptosis is complex, but in general, they are regulated reciprocally, with inhibitors of autophagy promoting apoptosis, perhaps by modulating mitochondrial pathways or mitophagy. Our findings indicate that CQ inhibits MC38 tumor cell autophagy. This effect may be related to induction of tumor cell apoptosis, given the complex interaction between the two processes. Addition of CQ to MC38 cells induced a significant dose-dependent increase in apoptotic cells, as demonstrated by Annexin V staining (Figure 7A). Increased cleaved caspase-3 and cleaved PARP production were found by western blotting (Figure 7B). Enhanced release of cytochrome C into the cytosol in CQ treated tumor cells was also observed by both western blot and immuno-fluorescent staining (Figures 7C and D). In aggregate, autophagy inhibition is indeed associated with induction of apoptosis in these cells.

Discussion

In the development of modern immunotherapy, experimentation in animal models has played an important role in advancing clinical trials in patients (38). Interestingly, the first murine tumor models used to demonstrate potent anti-tumor activity of IL-2 were methylcholanthrene-induced sarcomas with essentially no antitumor activity in humans with sarcomas. Similarly, although renal cancer and melanoma are the primary targets in humans, murine models show low activity of IL-2 alone in the Renca tumor model (although improved with the addition of IL-12 or IL-18) and with the nonimmunogenic murine melanoma, B16. It is perhaps best to consider, for many of these long-term cultured tumors, that the most important measure is of intrinsic immunogenicity rather than the tissue of origin. The liver is the primary site for metastasis in many epithelial tumors and, when unresectable, is associated with a high mortality rate. An hepatic model seems to more closely emulate metastases when compared with subcutaneous metastasis models (31). In this study, we established a reliable hepatic metastatic colorectal cancer model in mice using the intraportal route for injection. Using luciferase-labeled MC38 cells, enhanced tracking and better visualization of tumor growth is noted, allowing excellent correlation with data from pathologic examination and gross measurement of tumor bulk. This animal model permits sensitive detection and follow-up of hepatic metastases *in vivo*, allowing us to observe long term anti-tumor effects of HDIL-2 immunotherapy and perform mechanistic studies.

Although the precise mechanism(s) by which IL-2 mediates its anticancer effects is not fully understood, it is largely believed that it is affected by enhanced delivery to and activation of cytolytic effectors within tumor sites. Notwithstanding the presence of immune effectors, effective elimination of cancer often does not ensue, and the resistance has largely been attributed to effector dysfunction mediated by “exhaustion” (39) or the suppressive influences mediated by T regulatory cells (40) or myeloid derived suppressor cells (41). We have demonstrated that one of the major mechanisms of resistance resides in the target cells’ enhanced autophagy and resistance to apoptosis (42). Here we reported that administration of the autophagy inhibitor, CQ promotes substantial long-term antitumor effects when coupled with administration of IL-2. We also showed that IL-2 administration, in addition, causes not only release of HMGB1, a potent inducer of endogenous (33) and exogenous (43) autophagy, but also electron micrographic changes consistent with enhanced autophagy.

As a prototypic Damage Associated Molecular Pattern (DAMP) molecule, HMGB1 plays a central role in the pathogenesis of many inflammatory states released following tissue damage or injury, and is found in the serum including cancer (38-42) as well as other settings. In this model, we found that HMGB1 was released following HDIL-2 treatment and levels in the serum decreased following CQ treatment. We consider HMGB1 to be a likely candidate factor promoting the development of the ‘systemic autophagic syndrome’.

CQ has been used for over half a century in humans for the treatment of rheumatoid arthritis, SLE, HIV and malaria. CQ inhibits autophagy by blocking acidification of the lysosome, preventing fusion with the autophagosome (23). In a stressed cell, dependent on autophagy, this last step blockage results in increased generation of autophagosomes, eventually undergoing either apoptotic or necrotic cell death. Recently, several studies have shown that CQ has extensive biological effects, inhibiting cellular proliferation and/or inducing apoptosis in human and murine tumor cell lines such as the erythroleukemia K562 cells, breast cancer Bcap-37 cells (44), lung cancer A549 cells (27), ductal pancreatic adenocarcinoma cells, melanoma cells, C6 glioma cells (35), and mouse 4T1 cells. Autophagy inhibitors by themselves are unlikely to have significant clinical benefit, since only a small fraction of the tumor cells are under metabolic stress at a given time point. When combined with other chemotherapy agents, CQ enhanced cisplatin's cytotoxic effect and induced apoptosis by increasing the levels of intracellular misfolded proteins. In human cancer cell lines (24, 29) and murine models (30), CQ may exert significant antitumor activity by inhibiting the induction of autophagy following cancer therapy. CQ enhances chemotherapy and radiation sensitivity in clinical trials, the potential mechanisms underlying this enhancement are still unclear (45). Although Noman et al (20) have recently shown that CQ administration promotes the effectiveness of antitumor vaccines in a murine model, ours is the first demonstration that it enhances the effectiveness of a cytokine therapy. Here we also show that CQ limits autophagic vesicle degradation *in vitro* in two murine tumor cell lines. (Figure 5).

We demonstrated that CQ not only limited autophagy but also enhanced tumor cell apoptosis (Figure 7). Induction of apoptosis was associated with the loss of mitochondrial membrane potential, release of cytochrome c, and activation of caspase-9 and caspase-3, and cleavage of poly(ADP-ribose) polymerase. *In vivo*, CQ significantly inhibited 4T1 tumor growth and metastasis in murine models and induced apoptosis in the tumor microenvironment (28). Autophagy also plays an important role in the effector-target interactions of cytotoxic cells and can confer a survival advantage for tumor cells targeted for cytotoxic cell killing. Autophagy may contribute to tumor resistance and perhaps to the toxicity observed during IL-2 cancer therapy (46). Our results suggest that inhibition of autophagy with CQ in combination with HDIL-2 treatment can increase the antitumor effects and increase survival when compared with IL-2 treatment alone.

Several studies have suggested that autophagy may act as a protective mechanism in tumor cells in which cell death is induced by drugs, and that inhibition of autophagy provides antitumor effects alone (22-24) or synergistic effect with such drugs (25). The role of metabolism in cancer is increasingly being appreciated (47). With the notion that conventional oxidative phosphorylation is suppressed, replenishing anapleurotic production of Krebs cycle substrates, enabling anabolism, and cell division is necessary in stressed cells. Enhanced autophagy promotes degradation of intracellular substrates and allows generation of amino acids, nucleotides, and lipids that can promote and enable subsequent replication. Here we show that CQ (but not ethyl pyruvate) has the additional role of diminishing oxidative phosphorylation and limiting ATP production. This too may be part of the mechanism important in enhancing susceptibility in combination with IL-2 therapy.

Further work must evaluate the precise immunologic mechanisms operative in the IL-2 and CQ combination (Supplemental Figure 7), defining which immune effectors (T-cells or NK cells or both) have their activity promoted, whether autophagic inhibition limits immune reactivity through effects on dendritic cells, and define the precise role of HMGB1 in some of the biologic changes that we have demonstrated. To that end, we recently created floxed HMGB1 mice and are testing its elimination in pancreas, DCs, and NK cells. Recent studies (48) suggest that autophagy is required for the immunogenic release of ATP from dying tumor cells, and increased extracellular ATP release improves the efficacy of chemotherapy when autophagy is disabled. Further understanding of the complex biologic roles of metabolism, autophagy, and immune effectors will allow development of more effective and less toxic regimens for patients with cancer. We have initiated a clinical protocol to test the delivery of IL-2 with the CQ congener hydroxychloroquine in patients with advanced renal cell cancer based on these findings.

Supplementary Material

Refer to Web version on PubMed Central for supplementary material.

Acknowledgments

We would like to acknowledge Prometheus for the kind gift of IL-2. Dan Normolle in UPCI biostatistics was consulted for statistical and power considerations. We would like to give special thanks to our Cancer Center director, Nancy Davidson and the Department of Surgery Chairman, Timothy Billiar for supporting this work. The work was also supported by NIH P01 (CA 101944-04) and NCI core support P30CA047904.

Fiscal support: UPCI Cancer Center Support Grant, NIH 5P30 CA47904 (Nancy E. Davidson); NIH 1 P01 CA 101944 (Michael T. Lotze)

References

1. Clement JM, McDermott DF. The high-dose aldesleukin (IL-2) “select” trial: a trial designed to prospectively validate predictive models of response to high-dose IL-2 treatment in patients with metastatic renal cell carcinoma. Clin Genitourin Cancer. Aug; 2009 7(2):E7–9. [PubMed: 19692326]
2. Halama N, Zoernig I, Jaeger D. Advanced malignant melanoma: immunologic and multimodal therapeutic strategies. J Oncol. 2010; 2010:689893. [PubMed: 20224761]
3. Escudier B. Chemo-immunotherapy in RCC: the end of a story. Lancet. Feb 20; 2010 375(9715): 613–4. [PubMed: 20171385]
4. Dillman RO, Barth NM, VanderMolen LA, Fong WH, Mahdavi KK, McClure SE. Should high-dose interleukin-2 still be the preferred treatment for patients with metastatic renal cell cancer? Cancer Biother Radiopharm. Jun; 2011 26(3):273–7. [PubMed: 21711094]

5. Schwartzentruber DJ, Lawson DH, Richards JM, Conry RM, Miller DM, Treisman J, et al. gp100 peptide vaccine and interleukin-2 in patients with advanced melanoma. N Engl J Med. Jun 2; 2011 364(22):2119–27. [PubMed: 21631324]
6. Rosenberg SA, Yang JC, Sherry RM, Kammula US, Hughes MS, Phan GQ, et al. Durable Complete Responses in Heavily Pretreated Patients with Metastatic Melanoma Using T-Cell Transfer Immunotherapy. Clinical Cancer Research. Jul 1; 2011 17(13):4550–7. 2011. [PubMed: 21498393]
7. Hodi FS, O'Day SJ, McDermott DF, Weber RW, Sosman JA, Haanen JB, et al. Improved survival with ipilimumab in patients with metastatic melanoma. N Engl J Med. Aug 19; 2010 363(8):711–23. [PubMed: 20525992]
8. Maker AV, Phan GQ, Attia P, Yang JC, Sherry RM, Topalian SL, et al. Tumor regression and autoimmunity in patients treated with cytotoxic T lymphocyte-associated antigen 4 blockade and interleukin 2: a phase I/II study. Ann Surg Oncol. Dec; 2005 12(12):1005–16. [PubMed: 16283570]
9. George S, Pili R, Carducci MA, Kim JJ. Role of immunotherapy for renal cell cancer in 2011. J Natl Compr Canc Netw. Sep 1; 2011 9(9):1011–8. [PubMed: 21917625]
10. Finkelstein SE, Carey T, Fricke I, Yu D, Goetz D, Gratz M, et al. Changes in dendritic cell phenotype after a new high-dose weekly schedule of interleukin-2 therapy for kidney cancer and melanoma. J Immunother. Oct; 2010 33(8):817–27. [PubMed: 20842055]
11. Atkins MB, Lotze MT, Dutcher JP, Fisher RI, Weiss G, Margolin K, et al. High-dose recombinant interleukin 2 therapy for patients with metastatic melanoma: analysis of 270 patients treated between 1985 and 1993. J Clin Oncol. Jul; 1999 17(7):2105–16. [PubMed: 10561265]
12. Harris J. Autophagy and cytokines. Cytokine. Nov; 2011 56(2):140–4. [PubMed: 21889357]
13. Livesey KM, Tang D, Zeh HJ, Lotze MT. Autophagy inhibition in combination cancer treatment. Curr Opin Investig Drugs. Dec; 2009 10(12):1269–79.
14. Mathew R, White E. Autophagy in tumorigenesis and energy metabolism: friend by day, foe by night. Curr Opin Genet Dev. Feb; 2011 21(1):113–9. [PubMed: 21255998]
15. Ito H, Daido S, Kanzawa T, Kondo S, Kondo Y. Radiation-induced autophagy is associated with LC3 and its inhibition sensitizes malignant glioma cells. Int J Oncol. May; 2005 26(5):1401–10. [PubMed: 15809734]
16. Liang XH, Yu J, Brown K, Levine B. Beclin 1 contains a leucine-rich nuclear export signal that is required for its autophagy and tumor suppressor function. Cancer Res. Apr 15; 2001 61(8):3443–9. [PubMed: 11309306]
17. Ogier-Denis E, Houri JJ, Bauvy C, Codogno P. Guanine nucleotide exchange on heterotrimeric Gi3 protein controls autophagic sequestration in HT-29 cells. J Biol Chem. Nov 8; 1996 271(45): 28593–600. [PubMed: 8910489]
18. Proikas-Cezanne T, Waddell S, Gaugel A, Frickey T, Lupas A, Nordheim A. WIPI-1alpha (WIPI49), a member of the novel 7-bladed WIPI protein family, is aberrantly expressed in human cancer and is linked to starvation-induced autophagy. Oncogene. Dec 16; 2004 23(58):9314–25. [PubMed: 15602573]
19. Susan PP, Dunn WA Jr. Starvation-induced lysosomal degradation of aldolase B requires glutamine 111 in a signal sequence for chaperone-mediated transport. J Cell Physiol. Apr; 2001 187(1):48–58. [PubMed: 11241348]
20. Noman MZ, Janji B, Kaminska B, Van Moer K, Pierson S, Przanowski P, et al. Blocking hypoxia-induced autophagy in tumors restores cytotoxic T-cell activity and promotes regression. Cancer Res. Sep 15; 2011 71(18):5976–86. [PubMed: 21810913]
21. Kenific CM, Thorburn A, Debnath J. Autophagy and metastasis: another double-edged sword. Curr Opin Cell Biol. Apr; 2010 22(2):241–5. [PubMed: 19945838]
22. Dang CV. Antimalarial therapy prevents Myc-induced lymphoma. J Clin Invest. Jan; 2008 118(1): 15–7. [PubMed: 18097478]
23. Maclean KH, Dorsey FC, Cleveland JL, Kastan MB. Targeting lysosomal degradation induces p53-dependent cell death and prevents cancer in mouse models of lymphomagenesis. J Clin Invest. Jan; 2008 118(1):79–88. [PubMed: 18097482]
24. Zheng Y, Zhao YL, Deng X, Yang S, Mao Y, Li Z, et al. Chloroquine inhibits colon cancer cell growth in vitro and tumor growth in vivo via induction of apoptosis. Cancer Invest. Mar; 2009 27(3):286–92. [PubMed: 19194831]

25. Bellodi C, Lidonnici MR, Hamilton A, Helgason GV, Soliera AR, Ronchetti M, et al. Targeting autophagy potentiates tyrosine kinase inhibitor-induced cell death in Philadelphia chromosome-positive cells, including primary CML stem cells. J Clin Invest. May; 2009 119(5):1109–23. [PubMed: 19363292]
26. Yang C, Tong Y, Ni W, Liu J, Xu W, Li L, et al. Inhibition of autophagy induced by overexpression of mda-7/interleukin-24 strongly augments the antileukemia activity in vitro and in vivo. Cancer Gene Ther. Feb; 2009 17(2):109–19. [PubMed: 19730452]
27. Fan C, Wang W, Zhao B, Zhang S, Miao J. Chloroquine inhibits cell growth and induces cell death in A549 lung cancer cells. Bioorg Med Chem. May 1; 2006 14(9):3218–22. [PubMed: 16413786]
28. Jiang PD, Zhao YL, Deng XQ, Mao YQ, Shi W, Tang QQ, et al. Antitumor and antimetastatic activities of chloroquine diphosphate in a murine model of breast cancer. Biomed Pharmacother. Nov; 2010 64(9):609–14. [PubMed: 20888174]
29. Rahim R, Strobl JS. Hydroxychloroquine, chloroquine, and all-trans retinoic acid regulate growth, survival, and histone acetylation in breast cancer cells. Anticancer Drugs. Sep; 2009 20(8):736–45. [PubMed: 19584707]
30. Amaravadi RK. Autophagy-induced tumor dormancy in ovarian cancer. J Clin Invest. Dec; 2008 118(12):3837–40. [PubMed: 19033653]
31. Liang X, Chavez AR, Schapiro NE, Loughran P, Thorne SH, Amoscato AA, et al. Ethyl pyruvate administration inhibits hepatic tumor growth. J Leukoc Biol. Sep; 2009 86(3):599–607. [PubMed: 19584311]
32. Wack KE, Ross MA, Zegarra V, Sysko LR, Watkins SC, Stolz DB. Sinusoidal ultrastructure evaluated during the revascularization of regenerating rat liver. Hepatology. Feb; 2001 33(2):363–78. [PubMed: 11172338]
33. Tang D, Kang R, Livesey KM, Cheh CW, Farkas A, Loughran P, et al. Endogenous HMGB1 regulates autophagy. J Cell Biol. Sep 6; 2010 190(5):881–92. [PubMed: 20819940]
34. Hailey DW, Rambold AS, Satpute-Krishnan P, Mitra K, Sougrat R, Kim PK, et al. Mitochondria supply membranes for autophagosome biogenesis during starvation. Cell. May 14; 2010 141(4): 656–67. [PubMed: 20478256]
35. Geng Y, Kohli L, Klocke BJ, Roth KA. Chloroquine-induced autophagic vacuole accumulation and cell death in glioma cells is p53 independent. Neuro Oncol. May; 2010 12(5):473–81. [PubMed: 20406898]
36. Warburg O. On the origin of cancer cells. Science. Feb 24; 1956 123(3191):309–14. [PubMed: 13298683]
37. Kaelin WG Jr. Thompson CB. Q&A: Cancer: clues from cell metabolism. Nature. Jun 3; 2010 465(7298):562–4. [PubMed: 20520704]
38. Frampas E, Maurel C, Thedrez P, Remaud-Le Saec P, Faivre-Chauvet A, Barbet J. The intraportal injection model for liver metastasis: advantages of associated bioluminescence to assess tumor growth and influences on tumor uptake of radiolabeled anti-carcinoembryonic antigen antibody. Nucl Med Commun. Feb; 2011 32(2):147–54. [PubMed: 21116205]
39. Xiao X, Gong W, Demirci G, Liu W, Spoerl S, Chu X, et al. New Insights on OX40 in the Control of T Cell Immunity and Immune Tolerance In Vivo. J Immunol. Dec 5.2011
40. Amarnath S, Mangus CW, Wang JC, Wei F, He A, Kapoor V, et al. The PDL1-PD1 Axis Converts Human TH1 Cells into Regulatory T Cells. Sci Transl Med. Nov 30.2011 3(111):111ra20.
41. Kerkar SP, Goldszmid RS, Muranski P, Chinnasamy D, Yu Z, Reger RN, et al. IL-12 triggers a programmatic change in dysfunctional myeloid-derived cells within mouse tumors. J Clin Invest. Dec 1; 2011 121(12):4746–57. [PubMed: 22056381]
42. Kang R, Zeh HJ, Lotze MT, Tang D. The Beclin 1 network regulates autophagy and apoptosis. Cell Death Differ. Apr; 2011 18(4):571–80. [PubMed: 21311563]
43. Tang D, Kang R, Cheh CW, Livesey KM, Liang X, Schapiro NE, et al. HMGB1 release and redox regulates autophagy and apoptosis in cancer cells. Oncogene. Sep 23; 2010 29(38):5299–310. [PubMed: 20622903]
44. Jiang PD, Zhao YL, Shi W, Deng XQ, Xie G, Mao YQ, et al. Cell growth inhibition, G2/M cell cycle arrest, and apoptosis induced by chloroquine in human breast cancer cell line Bcap-37. Cell Physiol Biochem. 2008; 22(5-6):431–40. [PubMed: 19088425]

45. Amaravadi RK, Lippincott-Schwartz J, Yin XM, Weiss WA, Takebe N, Timmer W, et al. Principles and current strategies for targeting autophagy for cancer treatment. Clin Cancer Res. Feb 15; 2011 17(4):654–66. [PubMed: 21325294]

46. Romo de Vivar Chavez A, de Vera ME, Liang X, Lotze MT. The biology of interleukin-2 efficacy in the treatment of patients with renal cell carcinoma. Med Oncol. 2009; 26(Suppl 1):3–12. [PubMed: 19148593]

47. Romero-Garcia S, Lopez-Gonzalez JS, Baez-Viveros JL, Aguilar-Cazares D, Prado-Garcia H. Tumor cell metabolism: An integral view. Cancer Biol Ther. Dec 1.2011 12(11)

48. Michaud M, Martins I, Sukkurwala AQ, Adjemian S, Ma Y, Pellegatti P, et al. Autophagy-dependent anticancer immune responses induced by chemotherapeutic agents in mice. Science. Dec 16; 2011 334(6062):1573–7. [PubMed: 22174255]

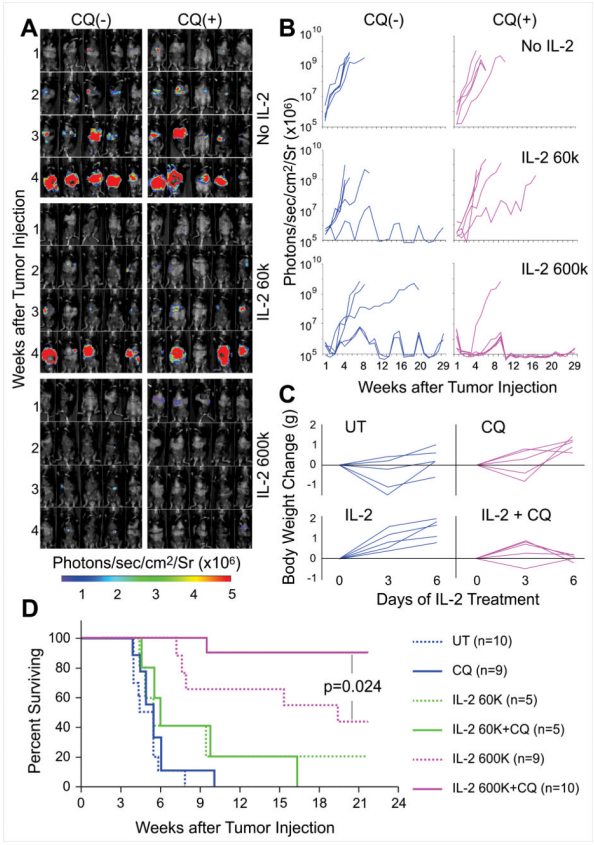

Figure 1. Chloroquine combination with rIL-2 markedly enhances anti-tumor effects, prolonging survival time in a murine hepatic metastasis model

C57BL/6 mice received 2×10^5/mouse luciferase expressing MC38 tumor cell via portal vein injection. On day 7 following tumor implantation, after an initial bioluminescence (BLI) measurement, mice were randomly divided into 6 groups and treated. Tumor growth was measured by BLI weekly and presented as the intensity of the luciferase signal. (A) BLI signals represents tumor development in individual animals (n=5/group) before (week 1, first row) and after treatment (week 2,3 and 4). Results shown are representative of three experiments. (B) Regions of interest were manually selected and quantification is reported as the average of photon flux within regions of interest. Each curve represents tumor development in a single mouse. Results shown are representative of three experiments. (C) Body weights were recorded every other day before and during treatment. The gains of body weight are compared with the body weight on the day before treatment. Each curve represents gain of body weight in individual mice. Administration of CQ prevents the gain of body weight in IL-2 treated mice ($p<0.05$) (D).Murine survival curve. When compared with the normal saline (untreated control, UT) group, HDIL-2 alone markedly prolonged survival time ($p<0.01$). CQ significantly enhanced HDIL-2 antitumor effects ($p=0.024$).

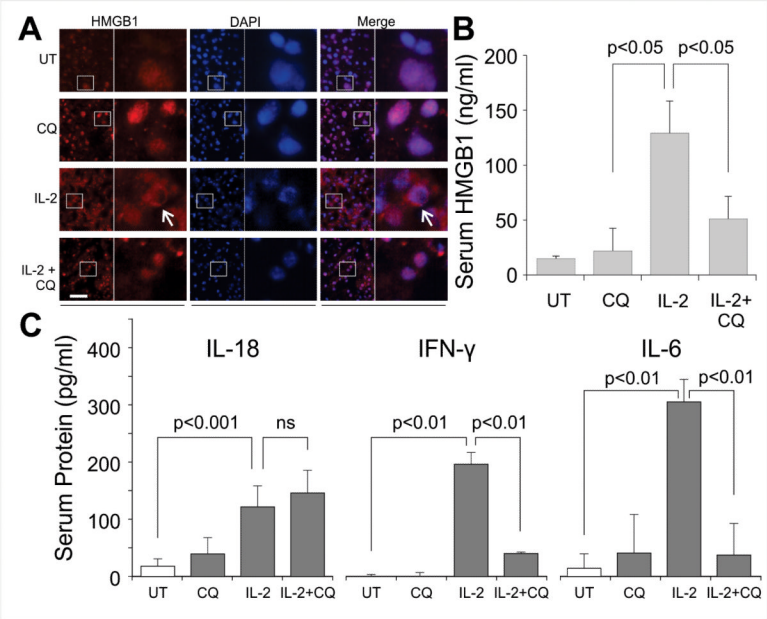

Figure 2. CQ decreases HMGB1 release that is stimulated by administration of IL-2

On day 12 following tumor cell inoculation, two hours after the last dose of IL-2 injection 3 mice from each group were sacrificed, livers and serum were harvested. (A) Immunofluorescence staining was performed using rat anti-human HMGB1 antibody (red) and DAPI nuclear staining (blue). HDIL-2 induced HMGB1 translocation from the nucleus into the cytoplasm in hepatocytes (arrow). HMGB1 was restricted in the nucleus with combination of CQ. Image represents 2 independent experiments using samples isolated from four individual mice. (B) Serum HMGB1 levels and (C) IL-6, IL-18 and IFN-γ were measured by ELISA and diminished after CQ administration (except IL-18). Results shown are representative of two independent experiments.

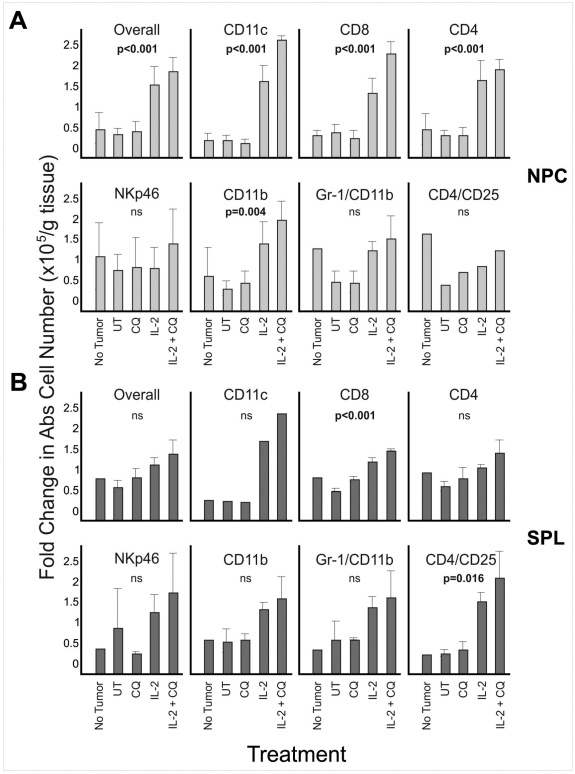

Figure 3. Administration of HDIL-2 and CQ stimulated immune cells proliferate and infiltrate into liver and spleen

Mononuclear cells from (A) livers and (B) spleens (3 mice /group) were isolated. Cell number were counted and normalized by tissue weight. Cells were stained with individual antibodies and analyzed by flow cytometry. Data shown are representative of one of three similar experiments performed. ANOVA p-values are shown for each set.

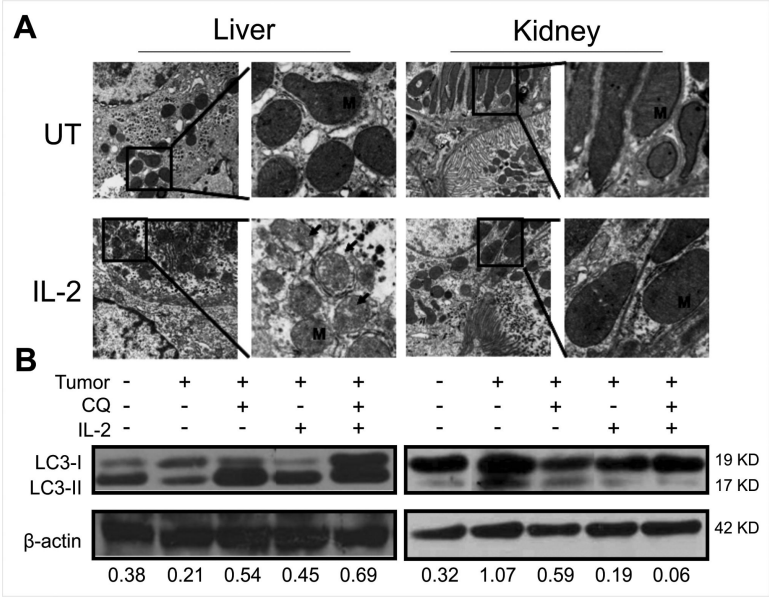

Figure 4. HDIL-2 administration promotes mitochondrial swelling and morphologic changes as well as autophagy *in vivo*

(A) Livers and kidneys were harvested from mice which received HDIL-2 (bottom row) treatment or UT (upper row) as a control. Ultrastructure of liver and kidney were observed under transmission electron microscopy (TEM). Damaged mitochondrial which exhibit plasma membrane disruption, absent and disordered mitochondrial christae (arrow) are observed in hepatocytes from IL-2 treated mice but not in control mice. The ultrastructure of a renal proximal tubule cell from both control and treated mice appear normal. (M indicates mitochondria). (B) Western blot analysis was performed in liver and kidney tissue lysates collected from tumor bearing mice which received IL-2 and /or in combination with CQ on the day after the last dose of IL-2 treatment (day 12). Enhanced autophagic flux was confirmed with increased LC-3 II levels. Numbers below represent LC3-II/actin ratio. Data are representative of one of three experiments.

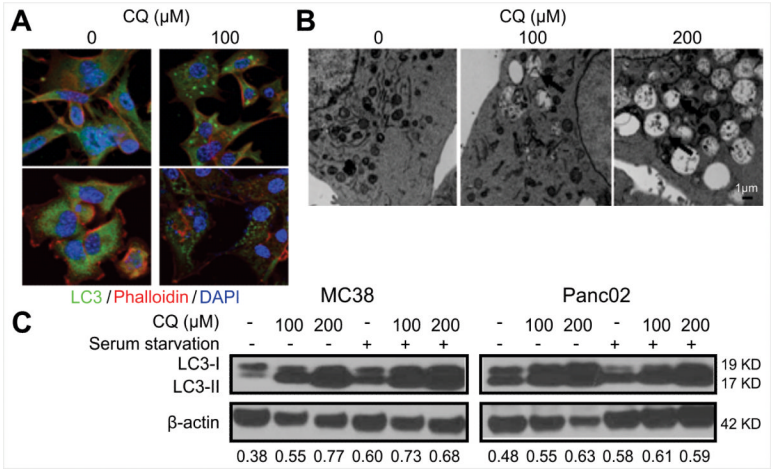

Figure 5. CQ inhibits autophagy in tumor cells *in vitro*

MC38 and Panc02 tumor cells were cultured and treated with 100 or 200μM CQ for 4 hour respectively. (A) Immunofluorence staining was performed for LC3 (green), actin (phalloidin, red) and nuclei (DAPI, blue). CQ increased LC3 punctae in both MC38 and Panc02 cells. (B) Ultrastructure of tumor cells was observed under TEM. An accumulation of autophagosomes (arrow) were observed in chloroquine treated cells. (C) Western blot analysis for LC3-I/II demonstrating a dose-dependent increase in MC38 tumor cells treated with CQ. Numbers shown below the Figure represent LC3-II/actin ratio. Data are representative of three experiments.

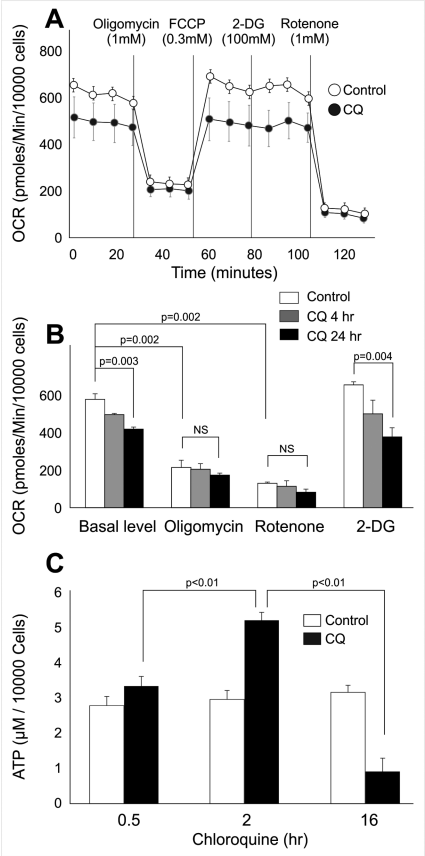

Figure 6. CQ alters tumor cell metabolism

(A) Oxygen consumption rate (OCR) was measured in real time in a Seahorse XF bioenergetic assay. 2×10^5 tumor cells were seeded with or without 100μM CQ for 4 hours. (B) Average OCR was calculated from 3 measurements during the treatment of each compound (oligomycin, FCCP, 2-DG, rotenone) at the concentration as indicated. (C) MC38 tumor cells were treated with 100μM CQ for the time indicated. Levels of ATP production were plotted as mean with standard deviations from experimental replicates..

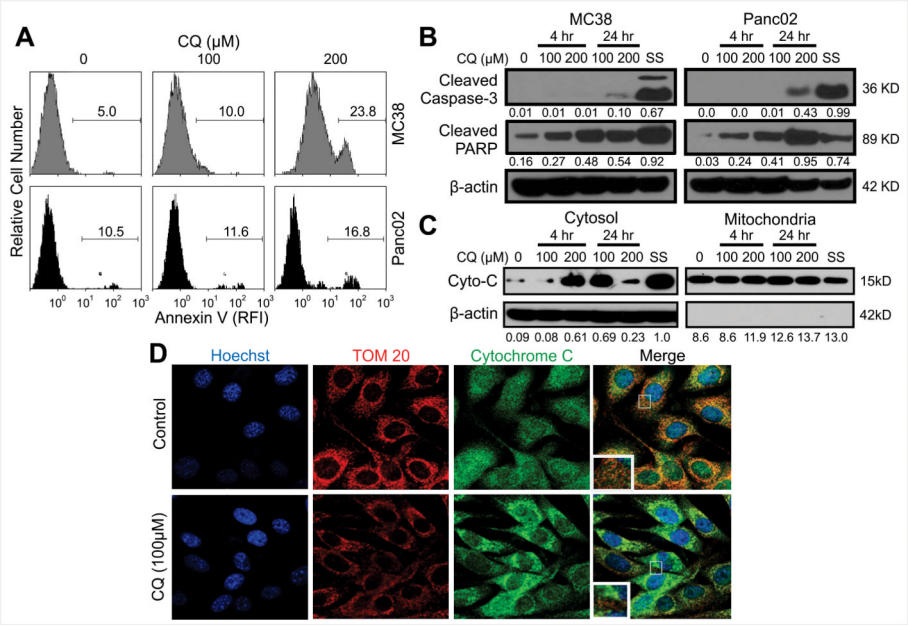

Figure 7. CQ induces tumor cell apoptosis associated with cytochrome C release from mitochondria

Tumor cell were cultured in the presence of 100 or 200 μM CQ for 4 hr or 24 hr before harvest. (A) Tumor cells exposed to 100 μM CQ for 4 hr and stained with Annexin V/PI were analyzed by flow cytometry. (B) Western blot analysis for cleaved PARP (C-PARP), cleaved caspase-3 demonstrating a dose-dependent increase in apoptosis of MC38 and Panc02 tumor cells treated with CQ. Numbers presented below each figure represent cleaved caspase 3/actin or cleaved PARP/actin ratio. Results shown are representative of three experiments. (C) Protein from mitochondria and cytosol of CQ treated MC38 cells were analyzed for cytochrome C by western blot analysis which demonstrated the release of cytochrome C from mitochondria into cytosol. Cells untreated or under serum starvation were used as controls. Numbers presented below each represent Cyt C/actin ratios. Results shown are representative of one of three experiments. (D) MC38 cells were treated with 100μM CQ for 24 hours then stained with cytochrome C (green), TOM-20 (mitochondrial marker, red) and Hoechst (blue). CQ treatment increases cytochrome C release.

Table 1

Combination CQ With HDIL-2 Prolongs Survival Time.

Group	n	Survival time (day)	Median survival time
PBS	10	27X3, 30, 31, 37, 38X2,40, 55	31
Chloroquine	9	27, 31, 33, 34, 38X2, 42X2, 70	38
rIL-2 60K IU	5	31, 33, 38, 66, >150	38
rIL-2 60K IU+CQ	5	32, 38, 43, 68, 114	43*
rIL-2 600K IU	9	50, 53, 55, 107, 135, >150x4	135**
rIL-2 600K IU +CQ	10	66, >150x9	150**??

Compare with PBS control group:

Compare with rIL-2 600KIU alone:

*p<0.05

**p<0.001

??p=0.02